Chapter 5

Materials Methodology and Experimental Program- Concrete

5.1 Introduction

This chapter presents a comprehensive overview of the study on concrete, covering materials, methodology, and the experimental program. Detailed scrutiny of the materials employed for concrete preparation is included herein. Additionally, the mix proportions for the concrete composition of MK and NS are furnished. A total of 8 distinct concrete compositions, encompassing binary and ternary MK and NS variants and a reference mix (normal concrete), were concocted. Moreover, the chapter delineates the executed experimental programs to assess concrete mechanical and durability attributes also thermal stability.

This section also expounds upon the techniques utilised for the microstructural characterisation of concrete samples. Microstructural analysis techniques, including Thermogravimetric Analysis (TGA), X-ray Diffraction (XRD), and Scanning Electron Microscopy (SEM), were employed to gain a comprehensive understanding of the internal characteristics of concrete. TGA was utilised to quantify the thermal stability and the decomposition behaviour of hydration products, while XRD facilitated the identification of crystalline phases, thereby enabling the assessment of hydration levels and the formation of specific compounds. SEM provided high-resolution imaging of the microstructure, revealing the morphology, phase distribution, porosity, and interactions between aggregates and the cement matrix. Collectively, these analyses provided critical insights into the concrete's durability, mechanical properties, and overall performance

5.2 Materials

The compositional constituents used in concrete formulation encompass OPC of 43 grade, MK and NS alongside fine and coarse aggregates and a superplasticizer (SP). The comprehensive exposition of OPC, MK, and CnS has been previously expounded upon in Chapter 3. Therefore, this session will only discuss fine and coarse aggregate and the SP.

5.2.1 Aggregates

Aggregates, comprising inert granular materials such as sand, gravel, or crushed stone, are integral to concrete alongside water and Portland cement. Their quality significantly impacts concrete properties, proportions, and economy. Clean, strong, hard aggregates devoid of chemicals or fine material coatings are essential. Fine aggregate, often natural sand or crushed stone, fills the voids in coarse aggregate. Gravels and crushed stones are primary constituents. Particle grading, shape, durability, absorption, and abrasion resistance are pivotal aggregate characteristics. Selection is crucial, affecting workability, strength, and longevity. Optimal grading and shape minimise water-cement ratio (w/c) adjustments, enhancing performance in diverse conditions.

i ***Coarse aggregate***

The locally available coarse aggregate consists of crushed basalt with a maximal particle size of 20 mm and complies with IS 383:1970 specifications. The aggregates retained by a 4.75 mm sieve include granular materials such as crushed stone. They form the basis of concrete when combined with granular aggregates and binders such as cement. The influence of coarse aggregates on the flowability, resistance to segregation, and strength of concrete is significant. Assessments of water absorption and specific gravity adhere to

IS 2386-1963 standards. Sieve analysis of the coarse aggregate of 20 mm and 10 mm is presented in Table 5.1 and Table 5.2, respectively. The physical properties of the aggregate are given in Table 5.4.

Table 5.1 Sieve analysis of 20 mm nominal size coarse aggregate

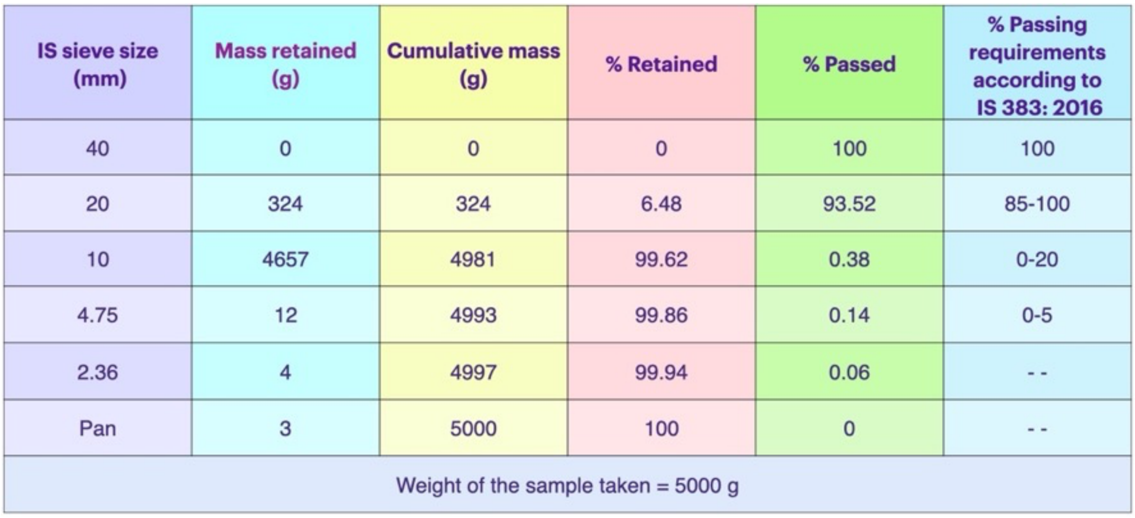

IS sieve size (mm)	Mass retained (g)	Cumulative mass (g)	% Retained	% Passed	% Passing requirements according to IS 383: 2016
40	0	0	0	100	100
20	324	324	6.48	93.52	85-100
10	4657	4981	99.62	0.38	0-20
4.75	12	4993	99.86	0.14	0-5
2.36	4	4997	99.94	0.06	- -
Pan	3	5000	100	0	- -
Weight of the sample taken = 5000 g					

Table 5.2 Sieve analysis of 10 mm nominal size coarse aggregate

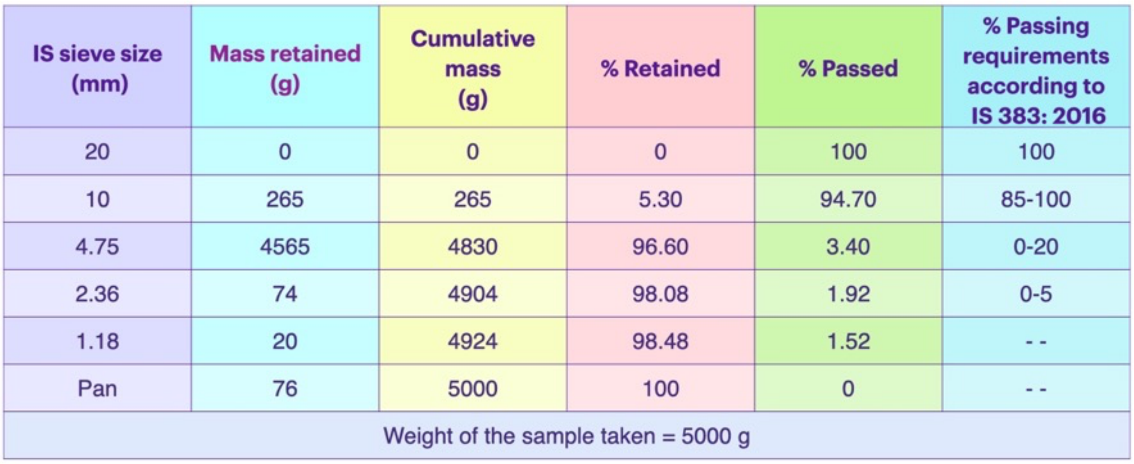

IS sieve size (mm)	Mass retained (g)	Cumulative mass (g)	% Retained	% Passed	% Passing requirements according to IS 383: 2016
20	0	0	0	100	100
10	265	265	5.30	94.70	85-100
4.75	4565	4830	96.60	3.40	0-20
2.36	74	4904	98.08	1.92	0-5
1.18	20	4924	98.48	1.52	- -
Pan	76	5000	100	0	- -
Weight of the sample taken = 5000 g					

ii ***Fine aggregate***

Fine aggregate refers to the aggregate that can pass through a 4.75 mm sieve but is retained on a 75 μm sieve, as defined by ASTM C125 [272] in 2004. It holds a vital role in concrete, significantly influencing the formulation of the mix. When utilised in appropriate ratios, fine aggregate enhances both the flowability of the mixture and its resistance to separation. Moreover, its incorporation in varying proportions alongside cement and coarse aggregate brings about alterations in the concrete's strength. Following IS 383:2016 [273], the sand chosen for this study originates from local sources and falls within Zone II criteria. The sieve analysis result of the fine aggregate is given in Table 5.3.

Table 5.3 Sieve analysis of fine aggregate

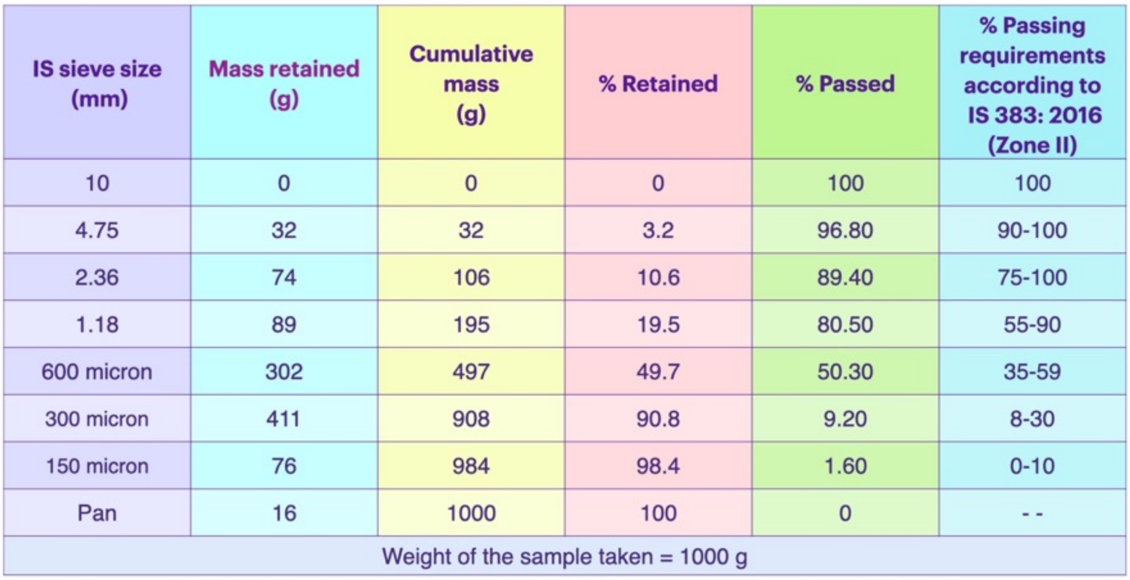

IS sieve size (mm)	Mass retained (g)	Cumulative mass (g)	% Retained	% Passed	% Passing requirements according to IS 383: 2016 (Zone II)
10	0	0	0	100	100
4.75	32	32	3.2	96.80	90-100
2.36	74	106	10.6	89.40	75-100
1.18	89	195	19.5	80.50	55-90
600 micron	302	497	49.7	50.30	35-59
300 micron	411	908	90.8	9.20	8-30
150 micron	76	984	98.4	1.60	0-10
Pan	16	1000	100	0	- -
Weight of the sample taken = 1000 g					

Several parameters, encompassing factors like the fineness modulus, moisture content, specific gravity, and sediment content of the sand, influence the proportions of the concrete blend. The fineness modulus represents a quantifiable factor determining the necessary fine aggregate quantity in a given mix design. Moisture content plays a crucial role in determining the mix proportions, dictating the volume of water that must either be introduced or removed from the blend. The higher specific gravity of fine aggregate contributes to the concrete's overall strength. If sand contains silt, it increases the requisite water volume for the concrete mixture while concurrently diminishing its strength. The physical properties of the fine aggreagate are given in Table 5.4.

Table 5.4 Physical properties of aggregates

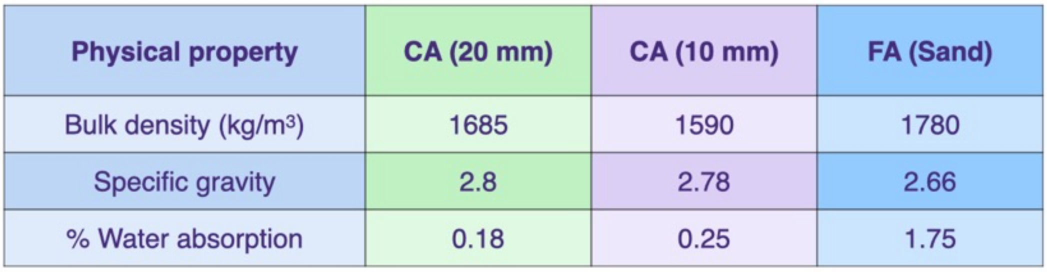

Physical property	CA (20 mm)	CA (10 mm)	FA (Sand)
Bulk density (kg/m^3)	1685	1590	1780
Specific gravity	2.8	2.78	2.66
% Water absorption	0.18	0.25	1.75

5.2.2 Water

Potable water from the IIT BHU campus with a temperature of 27±2ºC was used for preparing the mortar.

5.2.3 Superplasticiser

Superplasticisers (SP) play a pivotal role in enhancing the fluidity of concrete without resorting to increased water content. These agents create physical separation among cement particles by counteracting their natural attractive forces through steric or electrostatic mechanisms. Consequently, the process of concrete placement is greatly facilitated. This heightened workability endures for an extended period of at least 1.5 hours, rendering it advantageous for a spectrum of operations, including transportation, pouring, pumping, compaction, and casting. The manifold benefits bestowed by superplasticisers have rendered them indispensable constituents in modern concrete formulations. Notably, they offer the possibility to enhance workability while maintaining the critical water-to-binder (w/b) ratio, a determinant of concrete's durability and strength.

In scenarios where less reactive mineral admixtures substitute a fraction of cement, superplasticisers can effectively compensate for initial strength deficiencies. This feature bears implications for environmental sustainability, such as reducing cement consumption per unit of concrete volume in construction projects. Additional eco-friendly merits encompass diminished water usage, optimised concrete quantities to attain desired load-bearing capacities, and elongated service life through enhanced durability.

Superplasticisers are categorised based on their water-reducing efficacy: Lignosulfonates (LS) achieve approximately 10% reduction and find common utility in maintaining the workability of ready-mix concrete. Sulfonated naphthalene formaldehyde condensates (PNS) deliver up to 30% reduction and exhibit minimal interaction with clay constituents. Sulfonated melamine formaldehyde condensate (PMS) and polymelamine sulfonate (PMS) effectuate water reduction in the range of 20-30%. For the most substantial water reduction of up to 40%, synthetic polymers, including polycarboxylates and acrylic copolymers (PCEs), offer a route, albeit with slightly reduced clay tolerance.

Sika ViscoCrete 733-PR (Figure 5.1), a third-gen superplasticiser utilising polycarboxylate ether, was incorporated, with dosage adjusted based on binary and ternary concrete compositions. Table 5.5 summarises the superplasticiser's characteristics.

Figure 5.1 Sika ViscoCrete 733-PR

Table 5.5 Properties of superplasticiser

Superplasticizer	Sika ViscoCrete 733-PR
Chemical base	Modified polycarboxylate
Appearance/colour	Brown hazy liquid
Density	~ 1.10 kg/l at 25°C
pH - value	≥ 6
Approval/ standards	IS 9103, ASTM C494
**Provided by the manufacturer*	

5.3 Dosages of cementitious material for concrete

The substitution levels for MK and NS were determined based on the mortar performance of different blend combinations, as detailed in Chapter 4. Binary and ternary concrete compositions were formulated using 10% MK and 1.5%, 3%, and 4.5% NS, replacing the respective amount of OPC.

5.4 Mix design

The selection of concrete compositions and their corresponding proportions were based on the observed performance of the mortars investigated. An exhaustive examination of the mortars revealed a consistent k-factor of 1.53 at the 56-day mark when MK10 was introduced in concrete with 3% and 4.5% NS. Consequently, for the subsequent investigation on concrete, formulations comprising 10% MK in conjunction with 1.5%, 3%, and 4.5% NS were specifically chosen for the detailed study of their performance.

Table 5.6 Concrete mix proportion

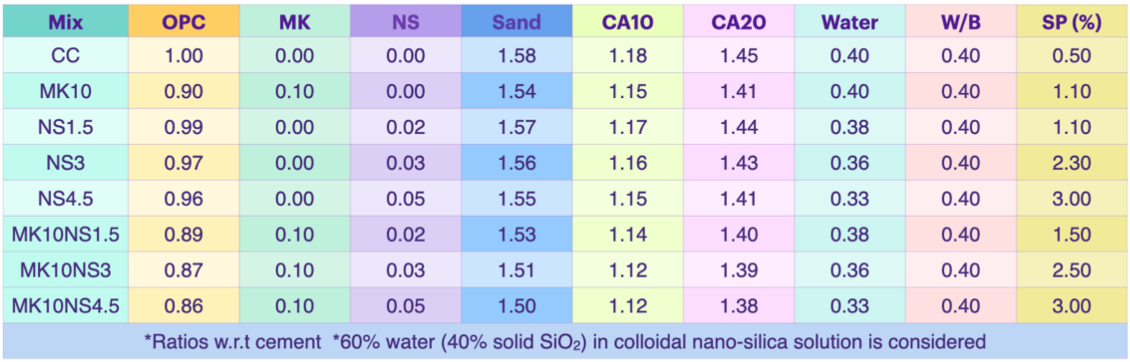

Mix	OPC	MK	NS	Sand	CA10	CA20	Water	W/B	SP (%)
CC	1.00	0.00	0.00	1.58	1.18	1.45	0.40	0.40	0.50
MK10	0.90	0.10	0.00	1.54	1.15	1.41	0.40	0.40	1.10
NS1.5	0.99	0.00	0.02	1.57	1.17	1.44	0.38	0.40	1.10
NS3	0.97	0.00	0.03	1.56	1.16	1.43	0.36	0.40	2.30
NS4.5	0.96	0.00	0.05	1.55	1.15	1.41	0.33	0.40	3.00
MK10NS1.5	0.89	0.10	0.02	1.53	1.14	1.40	0.38	0.40	1.50
MK10NS3	0.87	0.10	0.03	1.51	1.12	1.39	0.36	0.40	2.50
MK10NS4.5	0.86	0.10	0.05	1.50	1.12	1.38	0.33	0.40	3.00

*Ratios w.r.t cement *60% water (40% solid SiO_2) in colloidal nano-silica solution is considered

Determining the concrete mix formulation follows the guidelines specified in IS 10262: 2019 [274]. A water-to-binder ratio (w/b) of 0.40 was established. The targeted slump range for the mixtures ranged between 180 to 200 mm. The mix proportions for various concrete compositions are outlined in Table 5.6. The nomenclature for concrete samples follows a system where MK and NS, followed by the numerals, represent their replacement levels for cement in weight percentage; for instance, MK10NS1.5 denotes the concrete compositions with 10% MK and 1.5% NS in the mix. The reference, or normal concrete, is represented by CC.

5.5 Concrete mixing and casting of specimens

In the laboratory, preparing concrete mixtures involved employing a concrete mixer with a 100 kg capacity. First, cement and MK were meticulously combined manually in a pan until they were well integrated. Subsequently, the fine aggregate was introduced and thoroughly mixed until a uniform distribution of cementitious particles throughout the sand was achieved. The resulting blend of OPC, MK, and sand was transferred to a mixer containing a mixture of 10 and 20 mm coarse aggregates. A measured quantity of water was added to the mixer. Additionally, a colloidal silica solution, previously mixed with a portion of water, was introduced to the mixer, followed by the remaining water. The mixture was mixed thoroughly to attain concrete workability within the desired 180-200 mm slump range. The entire mixing procedure was completed within a span of 6 to 8 minutes.

Concrete cubes with dimensions of 100 mm (Figure 5.2a), prisms with dimensions of 500 mm x 100 mm x 100 mm (Figure 5.2b) and cylinders with dimensions of 100 mm in diameter and 200 mm in height (Figure 5.2c), were cast in a steel mould. The casting was followed by compaction on a vibrating table.

After casting, the cubes, prisms, and cylinders were subjected to a water curing process at a constant temperature of 27°C for 24 hours, after which they were extracted from their respective moulds. At 3, 7, 28, 90, and 180 days, the 100 mm cubes were used to determine the compressive strength of the concrete. These concrete cubes were also employed to assess durability parameters and the concrete's performance when exposed to elevated temperatures. The concrete prisms and cylinders were utilised to measure flexural and split tensile strengths at 28 days, respectively.

The flowchart of the blending and mixing process is shown in
Figure 5.3, illustrating the sequential order of the mixing stages.

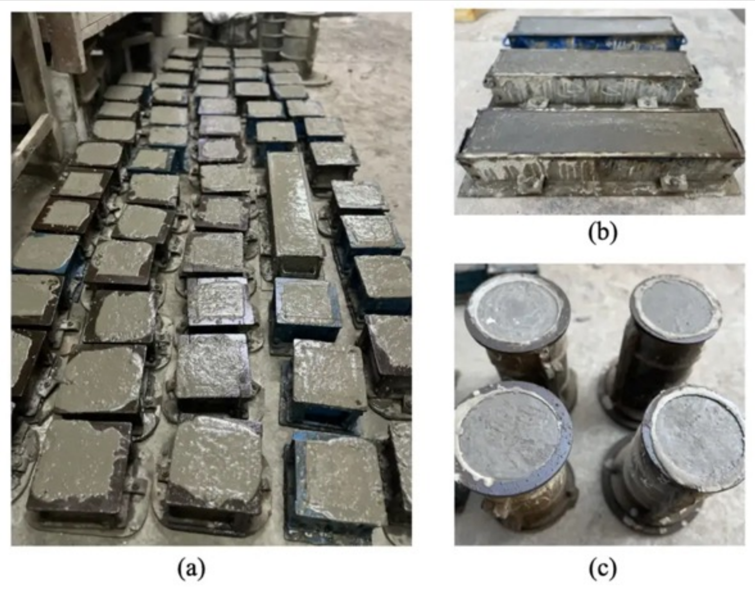

Figure 5.2 Cast concrete specimens, (a) cubes, (b) prisms, (c) cylinders

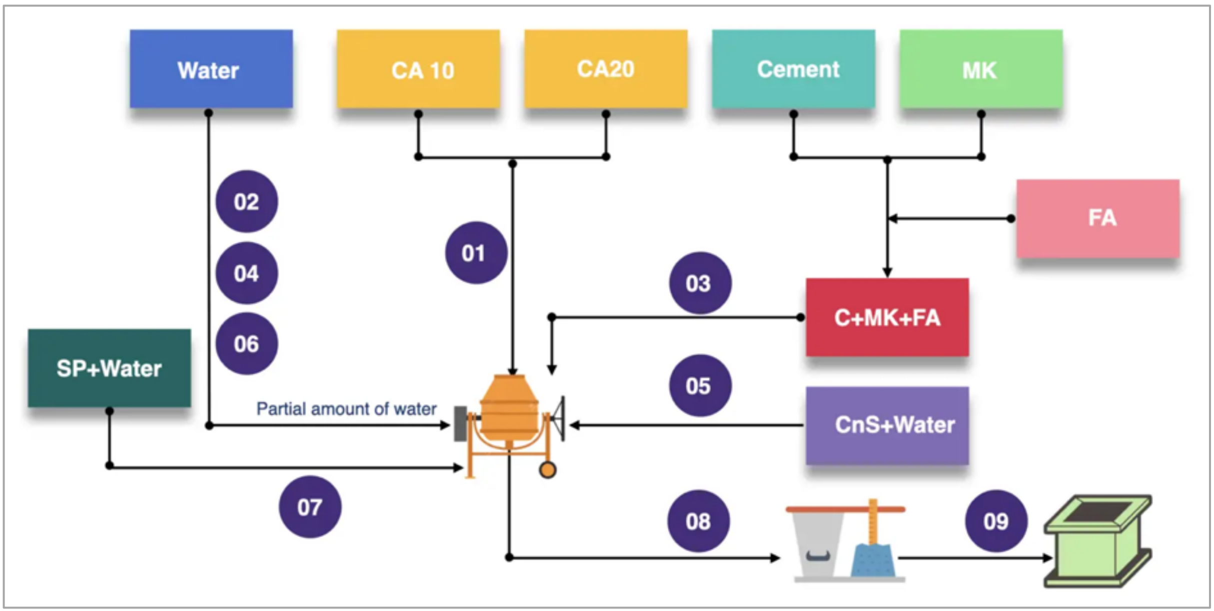

Figure 5.3 Concrete mixing process

5.6 Preparation of cement pastes

The cementitious pastes for microstructural investigations, encompassing normal cement and blends of MK and NS compositions, were formulated and processed as outlined in section 3.3.

5.7 Tests for mechanical properties

5.7.1 Compressive strength

Compression testing was conducted following the guidelines of IS 516 (Part 1/Sec 1): 2021 [275] on 100 mm concrete cubes. The compressive strength testing machine (AIMIL Ltd., Figure 5.4) used adhered to IS 14858: 2000 standards. The tests were carried out at various time intervals of 3, 7, 14, 28, 56, 90, and 180 days after curing. At each age, three specimens from each sample were subjected to testing. The average of these three measurements was considered the compressive strength for each batch.

After removal from the curing tank, the cubes were allowed to rest for 2 hours, during which excess moisture was eliminated from their surfaces. Subsequently, the cubes underwent testing. A consistent loading rate of 14 $N/mm^2/min$ was applied until the concrete cubes fractured. The compressive strength (f) is determined by the equation;

$$f = \frac{F}{A} \qquad \text{Equation 5.1}$$

Where f represents the compressive strength in MPa, F is the maximum load in N, and A is the cross-sectional area of the specimen in mm^2.

Figure 5.4 Compressive strength testing machine (Dept. of Civil Engineering, IIT BHU)

5.7.2 Split tensile strength

The split tensile strength test was conducted on cylindrical specimens with a diameter of 100 mm and a height of 200 mm. The testing procedure was performed using a compression testing machine (Figure 5.5) that adhered to the guidelines outlined in IS 14858: 2000 [276], following the specifications of IS 516 (Part 1/Sec 1): 2021[275]. After removal from the curing tank, the specimens were allowed to rest for 2 hours, during which excess moisture was eliminated from their surfaces. The tests were conducted on the specimens cured for 28 days. Three specimens from each sample were subjected to testing. The average of these three measurements was considered the split tensile strength for each batch.

The load application was executed smoothly, without sudden impact, and was incrementally increased at a consistent rate, falling within the 2 N/mm^2/min range until the specimen fractured. The utmost applied load during this process was duly documented. The resulting splitting tensile strength, denoted as fc, was determined through the subsequent formula:

$$f_c = \frac{2P}{\pi l d}$$ Equation 5.2

Where P is the maximum load applied to the specimen, in N; l is the length of the cylinder in mm; and d = diameter of the cylindrical specimen in mm.

Figure 5.5 Concrete cylinder specimens and testing

5.7.3 Flexural strength

Flexural strength testing was conducted on concrete specimens of size 100 mm x 100 mm x 500 mm conforming to IS 1199 (Part 5): 2018 standards [277]. These specimens were tested after 28 days of curing, following IS 516 (Part 1/Sec 1): 2021 [275] guidelines. After removal from the curing tank, the specimens were allowed to air dry for 2 hours to eliminate excess surface moisture.

A gradual and shock-free load application was employed to carry out the test, increasing continuously at a nominal rate of 1.8 kN/min until the specimen fractured. The maximum applied load was then recorded. The average of three measurements represented flexural strength. The flexural strength, F, was calculated using the following formula [275]:

$$F = \frac{PL}{bd^2}$$ Equation 5.3

Where *F* = Flexural strength in MPa, *P* = Maximum load in N, *b* and *d* = Lateral dimensions (breadth and height) of the specimen in mm and *L* = Length of the span on which the specimen is supported in mm.

Figure 5.6 Flexural strength test of concrete prism on the universal testing machine. (Dept. of Civil Engineering, IIT BHU)

5.8 Tests for durability parameters

5.8.1 Carbonation

After 28 days of water curing, 100 mm concrete cubes were subjected to accelerated carbonation in the carbonation chamber (Figure 5.7a). The carbonation chamber is designed to create a controlled environment in which concrete specimens are exposed to high concentrations of CO_2 by regulating relative humidity (RH) and temperature. The arrangement of the concrete cube inside the chamber is shown in

Figure 5.7b. The chamber can supply CO_2 up to 10% by volume, regulate temperature up to 30°C, and RH up to 99%.

The chamber's internal and external walls are made of stainless steel. The chamber includes three height-adjustable heavy-duty shelves constructed of stainless steel bars that can expose all the faces of the concrete cube to the environment within the chamber.

(a) (b)

Figure 5.7 (a) carbonation chamber, (b) arrangement of concrete cubes within the carbonation chamber (Dept. of Civil Engineering, IIT BHU)

The environment in the chamber in this investigation had a CO_2 concentration of 7.50±0.5% and a temperature of 27±2°C. The RH inside the chamber was kept at 70±5% to speed up the carbonation of concrete cubes. The concrete cubes were split after 14 and 28 days of exposure in the chamber, and the broken surfaces were sprayed with a standard mixture of 1% phenolphthalein in 70% ethyl alcohol. The indicator turned pink in the non-carbonated portion of the concrete cube with high alkalinity but remained colourless in the carbonated portion with low pH levels. The carbonation depth 'X' was calculated as the distance between the colour change boundary and the concrete surface. The depths at each sample's corners and behind the coarse aggregate were omitted. Several readings were taken from each of the four faces of the cubes, and the average of the readings from the two samples was taken to represent the specimen's carbonation depth (X) after 14 and

28 days of exposure to accelerated carbonation (t). The carbonation coefficients were determined by analysing the regression lines derived from the correlation between carbonation depth and the square root of time (carbonation period).

5.8.2 Water absorption

The water absorption test was conducted on the various concrete specimens after 28 days of curing. The rate of water absorption (sorptivity) by concrete was determined by measuring the increase in mass of a specimen as a function of time when only one surface of the specimen was exposed to water, as specified in ASTM C1585-13 [278]. The surface of the specimen is submerged in water, and water infiltration into unsaturated concrete is primarily influenced by capillary suction upon the initial stage of the contact of the surface with water.

For the water absorption test, the specimens were placed on a support in the pan to maintain the water level 1 to 3 mm above the top of the support, as seen in the test set-up shown in Figure 5.8. The 5 surfaces of the 100 mm cube specimens were sealed with plastic sheets and duct tape, as shown in Figure 5.9. The sealed specimens were weighed to the nearest 0.01 and recorded as the initial mass for water absorption calculations. The time and date of the initial contact of the specimen surface with water were recorded. The time was measured with the help of a stopwatch. The mass of the specimen was recorded at the time intervals shown in Table 5.7 after first contact with water, beginning at 60±2 s. Test samples were taken out of the pan for every mass measurement. A moist cloth was used to wipe away the excess surface water. Following the mass measurement, the specimen was replaced on the support in the pan and the stopwatch was restarted. The procedure was continued till the 9th day of the measurement.

The water absorption, A, is defined as the change in mass divided by the product of the specimen cross-sectional area and density of water, as expressed below.

$$A = \frac{m_t}{a \ X \ d} \qquad \text{Equation 5.4}$$

Where m_t is the change in mass of specimen in grams, at the time t; a is the area of the specimen exposed to water in mm^2 and d is the density of water in g/mm^3.

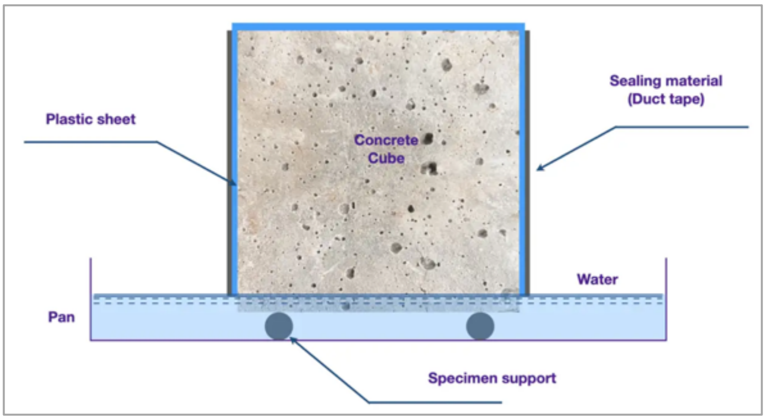

Figure 5.8 Schematic of water absorption test set-up

Figure 5.9 Experimental arrangement for water absorption test of concrete cubes

The timeline and respective allowable time tolerance for assessing water absorption, in accordance with ASTM C-1585-1, is shown in Table 5.7 and data gathering and computation format are outlined in Table 5.8.

The initial and secondary water absorption rates were determined through linear regression analyses. The slope of the line of best fit when plotting water absorption 'A' against the square root of time (√sec) is taken as the absorption rate. The initial rate (S_i) was calculated using data from 1 minute to 6 hours, while the secondary rate (S_s) used data points from 1 day to 7 days. Data points from which a significant change in slope were excluded from the analysis. If the data between 1 minute and 6 hours or 1 day and 7 days do not exhibit a linear relationship (correlation coefficient < 0.98) and show systematic curvature, it is impossible to determine the initial and secondary water absorption rates.

Table 5.7 Times and tolerance for water absorption test

Time	60s	5min	10min	20min	30min	60min	Every hour up to 6h	Once a day up to 3 days	Day 4 to 7, 3 measurements 24h apart	Day 7 to 9, 1 measurement 2h
Tolerance	2s	10s	2min	2min	2min	5min	2h	2h	2h	2h

Table 5.8 Data collection and calculation table format

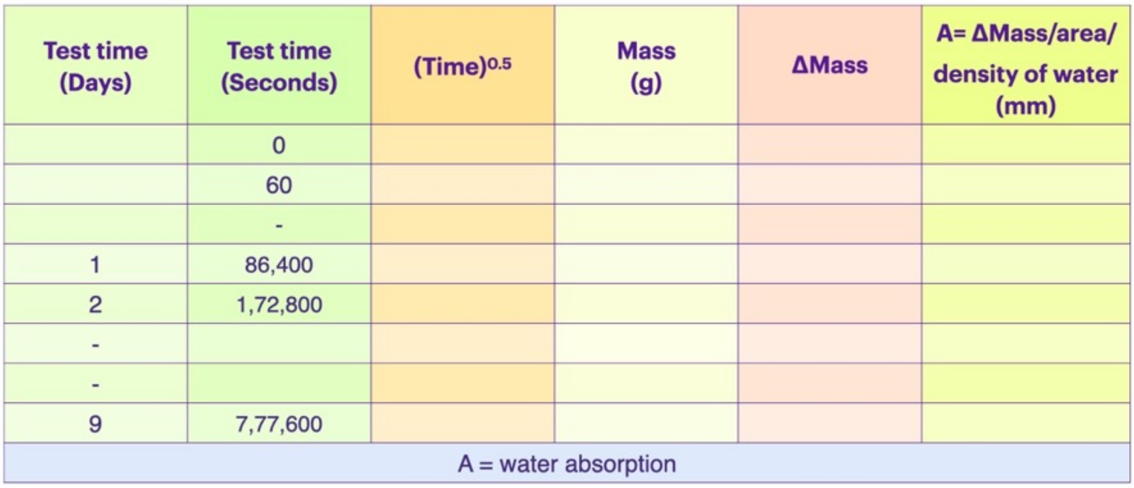

Test time (Days)	Test time (Seconds)	$(\text{Time})^{0.5}$	Mass (g)	ΔMass	A= ΔMass/area/ density of water (mm)
	0				
	60				
	-				
1	86,400				
2	1,72,800				
-					
-					
9	7,77,600				
A = water absorption					

5.8.3 Acid attack

Sulphuric acid (H_2SO_4) poses a significant threat to concrete structures due to its corrosive impact, resulting from both acid and sulfate attacks. The presence of significant sulfuric acid in industrial waste poses a risk to concrete structures in industrial areas, making them susceptible to sulfuric acid corrosion. The chemical reaction of sulfuric acid and CH produces gypsum, which causes an increase in the concrete volume. Moreover, gypsum's interaction with C3A results in the formation of ettringite, a compound that expands in volume sevenfold [279], creating internal pressure within the concrete and developing cracks [280]. Consequently, the corroded concrete experiences a reduced mechanical strength, leading to increased crack formation, spalling, and eventual complete structural deterioration [281]. The reaction of concrete when it comes in contact with sulfuric acid is expressed by Monteny et al. [279].

$$H_2SO_4 + Ca(OH)_2 \rightarrow CaSO_4.2H_2O \qquad \text{Equation 5.5}$$

Portlandite *Gypsum*

$$3(CaSO_4.2H_2O)+3CaO.Al_2O_3.12H_2O+14H_2O \rightarrow 3CaO.Al_2O_3.CaSO_2.32H_2O$$

(*Calcium aluminate hydrate)* (*Ettringite)* Equation 5.6

After curing for 28 days, two 100 mm cubes of each concrete composition were completely immersed in a 5% sulfuric acid solution with a pH of 1 (Figure 5.10). The mass loss of the concrete after the acid attack is a reliable indicator of its durability in aggressive environmental conditions. The initial mass M_i of each concrete cube specimen was recorded before immersing them in the solution using an electronic weighing scale with 0.5 resolution. The mass of the cubes, cured for 28 days, was recorded after oven drying at 100±5°C for 24 hours. These specimens were then allowed to remain in the solution for 28 days. To maintain a constant pH level, sulfuric acid was introduced to the solution every five days. After 28 days of immersion, the specimens were extracted from the solution, rinsed thoroughly with tap water, and delicately brushed using a wire brush to eliminate loose surface debris, if any. The samples were then dried at a temperature of 100±5°C for 24 hours, and the mass M_a after the acid attack was duly recorded.

The percentage of mass M_L was then calculated from the following expression.

$$M_L = \left(1 - \frac{M_i - M_a}{M_i}\right) x100 \qquad \text{Equation 5.7}$$

(a) (b)

Figure 5.10 Concrete cube in 5% sulfuric acid solution (a) day-1, (b) day-28

5.9 Thermal stability

The mechanical properties of the concrete at high temperatures can be assessed by three testing methods: transient or stressed test, steady-state or unstressed test, and residual or unstressed residual test. In the stressed test, the specimen is preloaded up to 40%

compressive strength at ambient temperature, heated at a constant rate to reach the desired temperature (target temperature), rested, and then loaded to failure. In the unstressed test, there is no preload; the specimen is heated at a constant rate, rested, and then loaded to failure. In the unstressed residual test, no preload is applied during heating, and the specimen is cooled before being loaded to failure. The unstressed residual method proves especially valuable for assessing concrete properties after exposure to high temperatures and fire. This study employed the unstressed residual test for its analysis.

A thermal stability test was conducted on 100 mm concrete cubes after 90 days of curing, recommended by the RILEM [159] to reflect the performance of real concrete structures at the fire. The concrete specimen in each composition was heated to five target temperatures of 200, 350, 500, 650 and 800°C. The heating process was performed in a muffle furnace (Figure 5.11), employing a heating rate of 10°C per minute and maintaining the desired temperature (target temperature) for two hours.

(a) (b) (c)

Figure 5.11 (a) Muffle furnace, (b) temperature level indicator, (c) concrete cubes in the furnace after heating (Dept. of Civil Engineering, IIT BHU)

The muffle furnace used in the experiment was equipped with a thermostat, which allowed precise control over the temperature and heating rate throughout the process. After the two-hour fixed-temperature exposure, the specimens were left at ambient temperature to cool down naturally. Following a 24-hour cooling period, load testing was conducted on the specimens. The heating, cooling and loading of concrete cubes were performed similarly to mortar cubes, as illustrated in Figures 3.11 and 3.12. To assess the concrete's response to high temperatures, the percentage mass loss of the cubes after heating was recorded by comparing it to their initial mass. Furthermore, an examination was performed on the cubes to determine the presence of surface cracks and spalling. TGA, XRD, and SEM techniques extensively investigated the microstructural details.

5.10 Microstructural studies

5.10.1 X-ray diffraction (XRD) analysis

The concrete samples underwent XRD analysis using the SmartLab X-ray diffractometer by Rigaku Co-Japan (Figure 5.12). Copper K**α** radiation (λ=1.5418 Å) was employed, and scanning occurred over a 2ø range spanning from 7º to 70º at a heating rate of 0.5°C per minute.

Powder of blended cement pastes for all compositions was used to identify the presence of hydrate. For XRD analysis of concrete exposed to high temperatures, the powder was extracted from cubes through grinding with mortar and pestles, ensuring the removal of fine and coarse aggregates. The powder was then sifted through an 80 µm mesh and dried at 40°C for 12 hours in an oven to eliminate moisture.

Figure 5.12 SmartLab X-ray diffractometer (Central instrumentation facility, IIT BHU)

The XRD analysis was performed on the cement paste, which had been cured for up to 28 days, to elucidate information regarding the hydrated products in the concrete. This analysis aimed to establish a correlation between the identified hydrated products and the compressive strength exhibited by the concrete at the 28-day curing. Additionally, XRD examinations were conducted on samples extracted from concrete cubes exposed to elevated temperatures of up to 800°C. This investigation sought to discern alterations in hydration products under varying temperature conditions, providing insights into the different concrete mixes' response to elevated thermal stresses.

5.10.2 Thermogravimetric and differential scanning calorimetry (TGA/DSC) analyses

Simultaneous TGA/DSC was carried out using an SDT-Q600 TA instrument (Figure 5.13) at Amrita Vishwa Vidyapeetham, Coimbatore. The finely ground samples, weighing around 2.5 to 3 mg and having a particle size below 80 µm, were heated under a nitrogen environment from 25 °C to 1000 °C at a rate of 10 °C/min. The same powders employed for XRD were utilised to perform TGA analysis, ensuring consistent and accurate results.

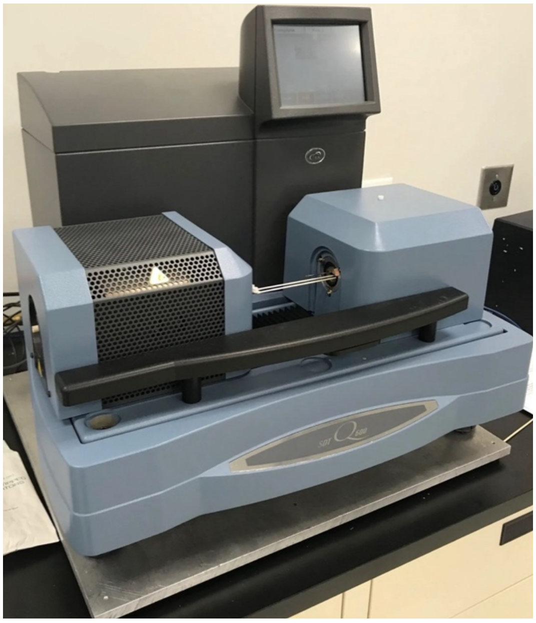

Figure 5.13 Simultaneous DSCTGA Q600-SDT (TA instrument)

TGA was executed on both 28-day and 90-day compositions of cement pastes and concrete powders extracted from carbonated samples. In the case of the 28-day cementitious samples, TGA results were compared with 28-day compressive strength, where mass loss during thermal decomposition is a direct indicator of hydration product quantity. The mass loss between 110°C and 650°C is attributed to hydration product dehydration, with higher mass loss indicating increased hydration product content. For the 90-day cement paste, TGA results offer insights into hydration product amounts at different temperature levels, correlating these mass losses with the compressive strength of concrete exposed to temperatures up to 800°C. TGA on carbonated samples reveals a quantity of $CaCO_3$ from the mass loss in the temperature range between 550°C and 950°C range, directly correlating to concrete carbonation.

5.10.3 Scanning electron microscopy (SEM)

The morphology of the hardened cement paste of unary, binary and ternary blended compositions was analysed using ZEISS EVO-18 high-magnification SEM (Figure 5.14a, Dept. of Geology, BHU). ZEISS GeminiSEM 300 (Figure 5.14b, Amrita Vishwa Vidyapeetham, Coimbatore) was used for the morphological study of the concrete subjected to elevated temperature. Before imaging, a sputter coating of gold was applied to the surface of the test sample to ensure the conductivity of the electron beam onto the sample.

SEM analysis was conducted on 28-day cured cementitious pastes and concrete powder derived from specimens exposed to elevated temperatures. The SEM images unveiled diverse hydration phases and illustrated the emergence of microcracks and voids within the microstructure of the concrete matrices, attributable to the high-temperature exposure.

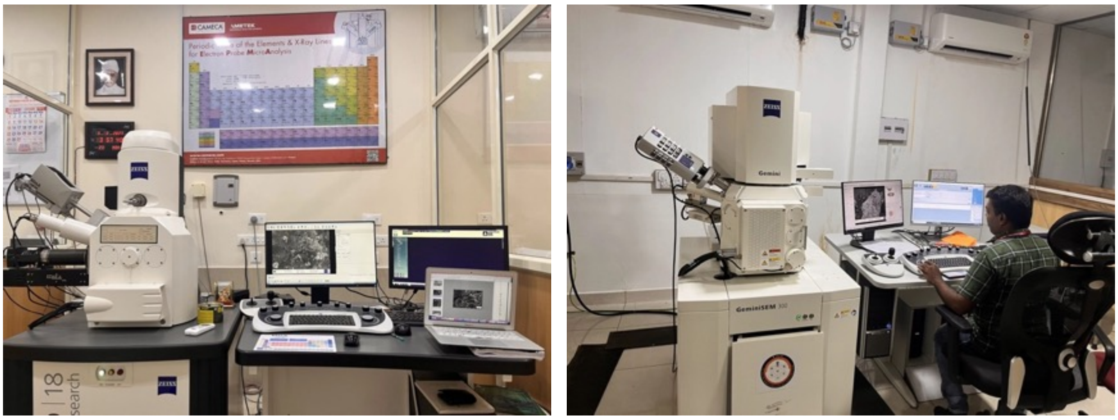

(a) (b)

Figure 5.14 (a) ZEISS EVO-18 high-magnification SEM (Dept. of Geology, BHU), (b) ZEISS GeminiSEM 300 (Amrita Vishwa Vidyapeetham, Coimbatore)

5.10.4 Porosity by N_2 adsorption

The crucial aspect of pore characterisation was undertaken through BET-BJH analysis using BELLSORP MAX II and BELCAT-II equipment from MicrotracBEL Corporation (Figure 5.15). The powdered cement paste samples, obtained by sieving through a 30-micron sieve, served as the basis for BET-BJH analysis. The BET method, relying on nitrogen adsorption, was employed to assess the specific surface area of the material, providing insights into monolayer gas adsorption. Subsequently, the BJH method, focusing on nitrogen desorption, facilitated determining pore size distribution, total pore volume and percentage porosity.

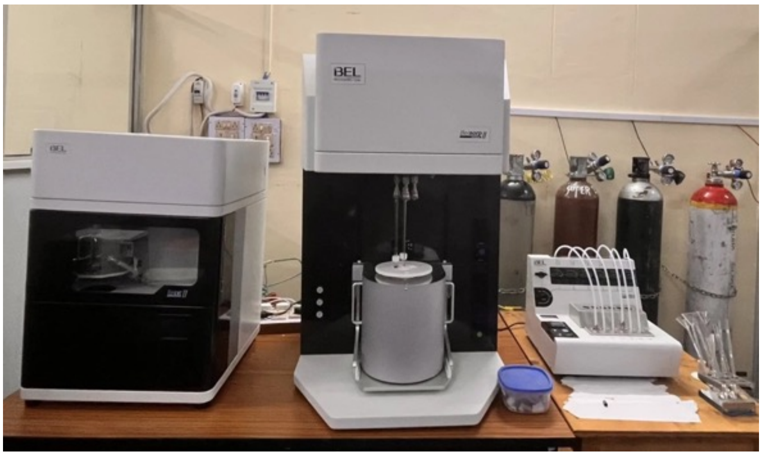

Figure 5.15 BET instrument (Central instrument facility, IIT BHU)

5.11 Summary

This chapter provided an extensive overview of concrete types, materials utilised in their formulation, mix proportions, and the methodologies for mixing, casting, and curing. The focus extended to the experimental procedures employed to investigate mechanical properties, encompassing compressive strength, split tensile strength, flexural strength, and durability performance concerning carbonation, water absorption, and acid attack. The chapter also delved into the examination of concrete's thermal stability. Furthermore, it addressed diverse techniques for microstructural analyses, such as XRD, TGA/DSC, BET/BJH, and SEM, elucidating their principles and processes.